Available online at www.sciencedirect.com
SCIENCE DIRECT®
Journal of Solid State Chemistry 176 (2003) 170–174
JOURNAL OF SOLID STATE CHEMISTRY
http://elsevier.com/locate/jssc

# Synthesis, crystal structure, and optical properties of $CeMn_{0.5}OSe$

Ismail Ijjaali, Kwasi Mitchell, Christy L. Haynes, Adam D. McFarland, Richard P. Van Duyne, and James A. Ibers*

*Department of Chemistry, Northwestern University, 2145 Sheridan Road, Evanston, IL 60208-3113, USA*

Received 11 March 2003; received in revised form 9 June 2003; accepted 3 July 2003

**Abstract**

The new quaternary selenide $CeMn_{0.5}OSe$ has been synthesized by the reaction of Ce, Mn, Se, and $SeO_2$ at 1223 K. This compound crystallizes in space group $P4/nmm$ of the tetragonal system with two formula units in a cell of dimensions at 153 K of $a = 4.0260(7)$ Å, $c = 9.107(2)$ Å. $CeMn_{0.5}OSe$ has the LaAgOS structure type. It is built from [CeO] fluorite-like layers where $Ce_4O$ tetrahedra share Ce–Ce edges that alternate with [MnSe] anti-fluorite like layers along [001]. An optical band gap of 2.01 eV has been derived from absorption measurements on the (100) crystal face of a $CeMn_{0.5}OSe$ single crystal.


*Keywords:* Cerium manganese oxyselenide; Synthesis and X-ray structure; Band gap

## 1. Introduction

Numerous quaternary oxychalcogenides involving 4*f* elements and 3*d* transition metals have been identified. In most of these phases there is an early transition element and a light lanthanide (La, Ce, Pr, Nd, Sm). These include titanium oxysulfides $La_6Ti_2O_5S_8$ [1], $La_4Ti_3O_8S_4$ [1], $Ln_{20}Ti_{11}O_6S_{44}$ ($Ln$ = La, Ce) [2,3], $La_{14}Ti_8O_6S_{33}$ [4], $La_8Ti_{10}O_4S_{24}$ [5], $La_{8+x}Ti_{8+y}O_4S_{24}$ ($x+y \leqslant 2$) [6], $Ln_2Ti_2O_5S_2$ ($Ln$ = Pr, Nd, Sm) [7,8], and the recently synthesized titanium oxyselenides $Ln_{3.67}Ti_2O_3Se_6$ ($Ln$ = Ce, Nd, Sm) [9], $Sm_3Ti_3O_8Se_2$ [10], $La_4Ti_2O_4Se_5$ [11], and $La_6Ti_3O_5Se_9$ [11]. The only two vanadium representatives are $Ln_5V_3O_7S_6$ ($Ln$ = La, Ce, Pr, Nd) [12,13] and $Ln_7VO_4Se_8$ ($Ln$ = Nd, Sm, Gd) [14]. If one assumes $Ln^{3+}$, then some of these phases are mixed-valence compounds because they contain no $Q$–$Q$ bonds ($Q$ = S, Se). In the chromium system $LnCrOQ_2$ ($Q$ = S; $Ln$ = La, Ce, Pr, Nd, Sm [15–18]; $Q$ = Se; $Ln$ = La, Ce, Nd [19,20]) ferromagnetic ordering occurs in $LaCrOQ_2$ ($Q$ = S, Se) and antiferromagnetic interactions occur in $NdCrOS_2$ [19].

These $Ln/M/O/Q$ compounds ($M$ = Ti, V, Cr) display three-dimensional crystal structures comprising face- and edge-sharing of polyhedra. Layered structures have been observed only with $M$ = Cu in $LnCuOQ$ ($Q$ = S; $Ln$ = La [21]; $Q$ = Se; $Ln$ = La, Pr, Nd, Sm, Gd, Dy, Y [22–24]) and more recently in $La_5Cu_6O_4S_7$ [25].

Our interest in the preparation of new phases that contain other transition metals led us to explore the $Ln$/Mn/O/Se system, where we have been able to isolate single crystals of the first quaternary cerium oxyselenide that involves manganese, $CeMn_{0.5}OSe$, the subject of the present paper.

## 2. Experimental

### 2.1. Synthesis

A few dark-orange plates of $CeMn_{0.5}OSe$ were obtained in the reaction of Ce (2 mmol, Alfa, 99.9%), Mn (1 mmol, Alfa, 99.9%), Se (4 mmol, Alfa, 99.5%), $SeO_2$ (0.5 mmol, Aldrich, 99.8%) added as source of oxygen, and KCl (5 mmol, Aldrich, 99.9%) added to promote crystal growth. The materials were mixed and sealed in a fused-silica tube that was then evacuated to $5 \times 10^{-5}$ Torr. The tube was heated to 1223 K at 0.25 K/min, kept at 1223 K for 5 days, cooled at 0.05 K/min to 923 K, and then the furnace was turned off. The reaction mixture was washed free of chloride salts with water and then dried with acetone. Yield of $CeMn_{0.5}OSe$ crystals was about 5%; the composition of

*Corresponding author. Fax: +1-847-491-2976.
*E-mail address:* ibers@chem.northwestern.edu (J.A. Ibers).

0022-4596/$ - see front matter © 2003 Elsevier Inc. All rights reserved.
doi:10.1016/S0022-4596(03)00385-2

the bulk powder was not determined. Semiquantitative analyses of the crystals were performed with a Hitachi 3500N SEM. EDX results confirmed the presence of Ce, Mn, and Se in the approximate ratio 2:1:2, in good agreement with the final formulation based on the X-ray structure determination. Oxygen was detected but could not be quantified. This compound is stable in a laboratory atmosphere.

### 2.2. Crystallography

Single-crystal X-ray diffraction data were collected on a plate of dimensions 0.052 mm × 0.070 mm × 0.014 mm with the use of graphite-monochromatized Mo$K\alpha$ radiation ($\lambda = 0.71073$ Å) at 153 K on a Bruker Smart-1000 CCD diffractometer [26]. The crystal-to-detector distance was 5.023 cm. Crystal decay was monitored by recollecting 50 initial frames at the end of data collection. Data were collected by a scan of 0.3° in $\omega$, respectively, in groups of 606, 606, 606, and 606 frames at $\varphi$ settings of 0°, 90°, 180°, and 270°. The exposure times were 20 s/frame. The collection of intensity data on the Bruker diffractometer was carried out with the program SMART [26]. Cell refinement and data reduction were carried out with the use of the program SAINT [26] and a face-indexed absorption correction was performed numerically with the use of the program XPREP [27]. The program SADABS [26] was then employed to make incident beam and decay corrections.

The structure was solved and refined in the tetragonal space group *P4/nmm*. The positions of the heavy atoms (Ce, Mn, Se) were determined by direct methods with the program SHELXS of the SHELXTL suite of programs [27] and then the O atom position was located from a difference electron density synthesis. The structure was refined by full-matrix least-squares techniques with the use of the program SHELXL [27]. The resultant equivalent isotropic displacement parameter for Mn was excessively large, indicating that there was less electron density at this site than that assumed in the refinement model of CeMnOSe. Refinement with unconstrained occupancy for Mn led to a reasonable displacement parameter and to an occupancy of 0.5. Final refinement with this occupancy fixed at 0.5 led to the agreement indices $R = 0.0190$ and $R_w = 0.0493$. The resultant stoichiometry of $CeMn_{0.5}OSe$ achieves charge balance with the formal oxidation states $Ce^{3+}Mn^{2+}_{0.5}O^{2-}Se^{2-}$. Additional experimental details are given in Table 1. The program STRUCTURE TIDY [28] was used to standardize the positional parameters. Fractional coordinates and equivalent isotropic displacement parameters are listed in Table 2, and selected interatomic distances and bond angles are given in Table 3.

Table 1
Crystal data and structure refinement for $CeMn_{0.5}OSe$

| | |
|---|---|
| Formula weight | 262.55 |
| Space group | *P4/nmm* |
| $a$ (Å) | 4.0260(7) |
| $c$ (Å) | 9.107(2) |
| $V$ (Å$^3$) | 147.61(5) |
| $Z$ | 2 |
| $T$ (K) | 153 (2) |
| $\lambda$ (Mo$K\alpha$) | 0.71073 |
| $\rho_c$ (g/cm$^3$) | 5.907 |
| $\mu$ (cm$^{-1}$) | 294.73 |
| Transmission factors | 0.212–0.664 |
| Total reflections/unique reflections | 1240/143 |
| $R(F)^a$ ($F_o^2 > 2\sigma(F_o^2)$) | 0.0190 |
| $R_w$ ($F_o^2$)$^b$ (all data) | 0.0493 |

[a] $R(F) = \sum||F_o| - |F_c||/\sum|F_o|$.
[b] $R_w(F_o^2) = [\sum w(F_o^2 - F_c^2)^2/\sum wF_o^4]^{1/2}$, $w^{-1} = \sigma^2(F_o^2) + (0.02 \times F_o^2)^2$ for $F_o^2 > 0$; $w^{-1} = \sigma^2(F_o^2)$ for $F_o^2 \leqslant 0$.

Table 2
Atomic coordinates and equivalent isotropic displacement parameters for $CeMn_{0.5}OSe$

| Atom | $x$ | $y$ | $z$ | $U_{eq}$[a] |
|---|---|---|---|---|
| Ce | 1/4 | 1/4 | 0.63386(6) | 0.0095(2) |
| Mn[b] | 3/4 | 1/4 | 0 | 0.0107(6) |
| O | 3/4 | 1/4 | 1/2 | 0.0086(13) |
| Se | 1/4 | 1/4 | 0.17655(12) | 0.0109(3) |

[a] $U_{eq}$ is defined as one-third of the trace of the orthogonalized $U_{ij}$ tensor.
[b] Occupancy = 0.5.

Table 3
Selected interatomic distances (Å) and angles (deg) for $CeMn_{0.5}OSe$

| | | | |
|---|---|---|---|
| Ce–O × 4 | 2.3533(5) | Ce–O–Ce × 4 | 74.435(13) |
| Ce–Se × 4 | 3.3295(8) | Ce–O–Ce × 2 | 117.60(3) |
| Mn–Se × 4 | 2.5763(8) | Se–Mn–Se × 4 | 112.92(2) |
| Mn···Mn × 4 | 2.8468(5) | Se–Mn–Se × 2 | 102.77(4) |

### 2.3. Optical properties

Optical absorption measurements on a $CeMn_{0.5}OSe$ single crystal were performed with the use of an Ocean Optics model S2000 spectrometer over the range 400 nm (3.10 eV) to 800 nm (1.55 eV) at 293 K. The spectrometer was coupled by fiber optics to a Nikon TE300 inverted microscope. White light originated from the TE300 lamp and passed through a polarizer before reaching the sample. The crystal, aligned along [010], was positioned at the focal point above the 20 × objective by means of a goniometer mounted on translation stages (Line Tool Company). The light transmitted through the crystal was then spatially filtered before being focused into the 400 μm core diameter fiber coupled to the spectrometer. Fine alignment of the microscope assembly was achieved by maximizing the transmission of the lamp profile. The extinction spectrum of the (100) crystal plane (light in the [100] direction) was recorded. Owing

to the dimensions of the crystal, the extinction spectrum of the (001) crystal plane could not be obtained. The direct band gap ($E_g$) for $CeMn_{0.5}OSe$ was calculated according to the relation $(\alpha hv)^2 \sim hv - E_g$, where $\alpha$ is the molar absorption coefficient and $hv$ is the incident photon energy. The molar absorption coefficient was corrected to account for crystal thickness and the probe spot fill factor. Then $E_g$ was calculated by extrapolation to $(\alpha hv)^2 = 0$. A detailed description of the band gap calculation procedure was given previously [29].

## 3. Results and discussion

### 3.1. Synthesis

$CeMn_{0.5}OSe$ was synthesized in very low yield in the reaction of Ce, Mn, Se, and $SeO_2$ at 1223 K. Attempts to improve the yield were unsuccessful.

### 3.2. Structures

The unit cell of $CeMn_{0.5}OSe$ displayed down [100] is shown in Fig. 1. This compound belongs to the layered phases crystallizing in the LaAgOS structure type [30]. The structure of $CeMn_{0.5}OSe$ is built from [CeO] fluorite-like layers where $Ce_4O$ tetrahedra share Ce–Ce edges that alternate with [MnSe] anti-fluorite like layers along [001]. The distance between the [CeO] layers is 6.670 Å. The distance between two [MnSe] layers is 5.892 Å.

Several views of the structure showing the coordination polyhedra of Ce, Mn, Se, and O are presented in

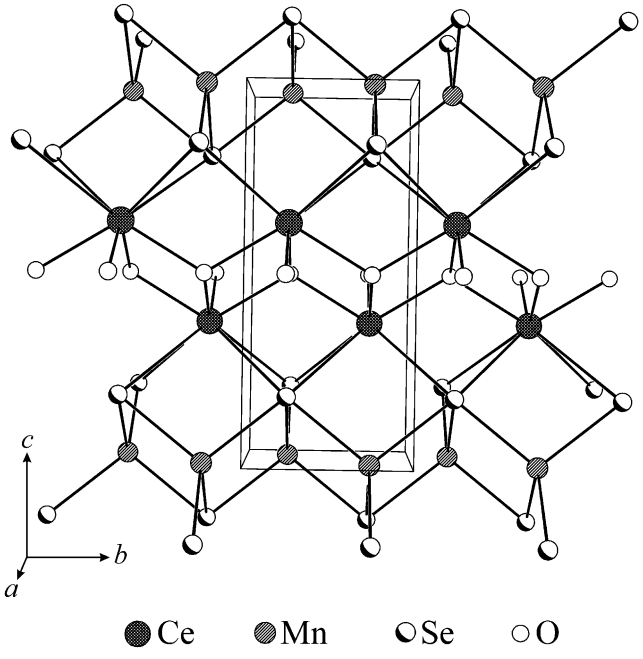


Fig. 1. Unit cell of $CeMn_{0.5}OSe$ viewed down [100].

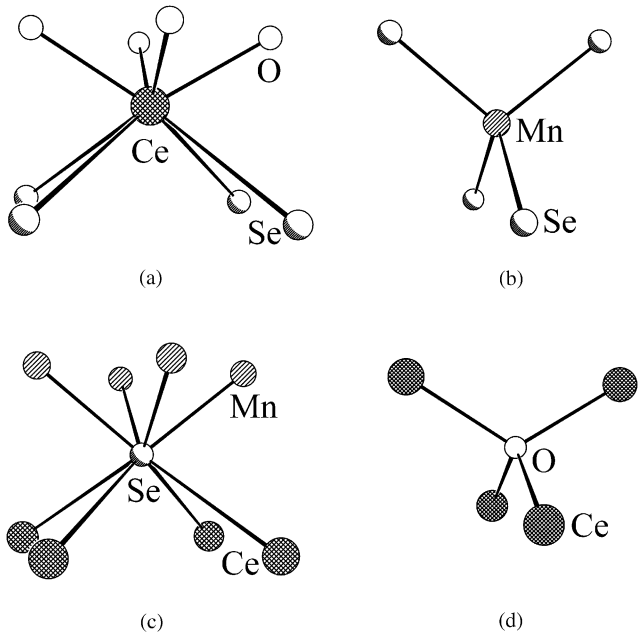


Fig. 2. Atomic environments in $CeMn_{0.5}OSe$.

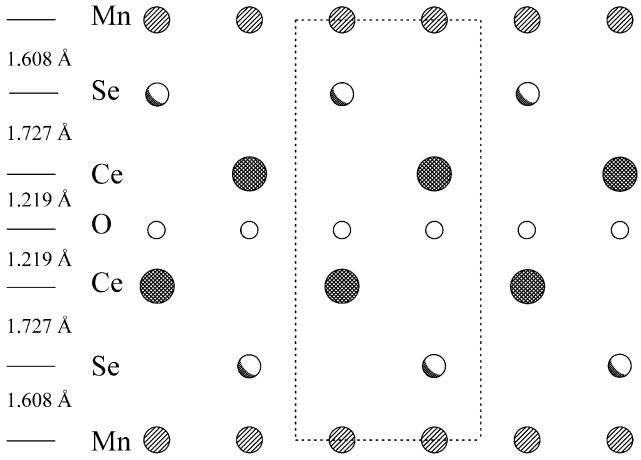


Fig. 3. Interlayer distances in $CeMn_{0.5}OSe$.

Fig. 2. The coordination polyhedron of Ce is a distorted square antiprism comprising four O atoms in one base and four Se atoms in the other. The height of this $Se_4O_4$ antiprism is 2.946 Å, where Ce is situated 1.219 Å from the O base and 1.727 Å from the Se base (Fig. 3). The coordination polyhedron of Se is also a distorted square antiprism with four Mn atoms in one base and four Ce atoms in the other. The height of the $Mn_4Ce_4$ antiprism is 3.335 Å, where the Se atom is located at 1.608 Å from the Mn base and 1.727 Å from the Ce base. Each O atom is coordinated by four Ce atoms in a distorted tetrahedral arrangement. Each Mn atom is coordinated tetrahedrally to four Se atoms; the $MnSe_4$ tetrahedra share edges to form the [MnSe] anti-fluorite like layer.

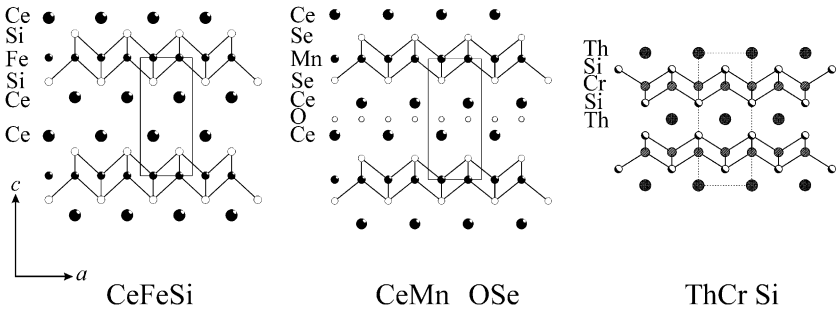


Fig. 4. Structural relationships among the CeFeSi, $CeMn_{0.5}OSe$, and $ThCr_2Si_2$ structures.

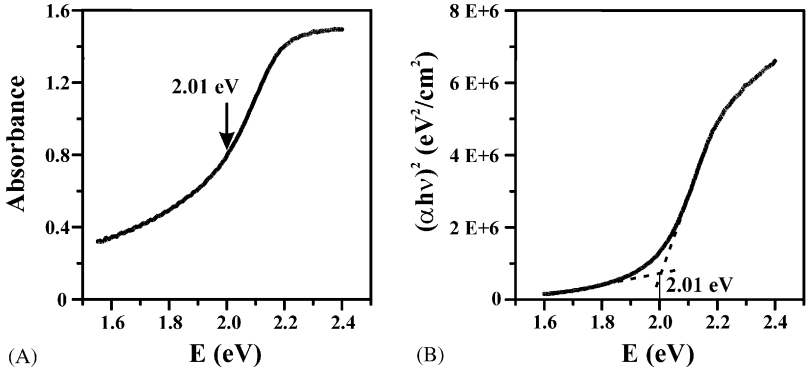


Fig. 5. Optical absorption spectrum (A) and band gap calculation (B) for $CeMn_{0.5}OSe$. The light impinged on the (100) crystal face.

The Ce–O distance of 2.3533(5) Å and the Ce–Se distance of 3.3295(8) Å are comparable to those in $Ce_4(Si_2O_7)Se_3$ (Ce–O, 2.399–2.545 Å; Ce–Se, 2.991–3.483 Å) [31] and those in $CeCrOSe_2$ (Ce–O, 2.354–2.428 Å; Ce–Se, 3.146–3.255 Å) [20]. The Mn–Se distances of 2.5763(8) Å agree well with those reported in the literature for Mn in tetrahedral coordination, e.g., 2.524–2.601 Å in $Ba_2MnSe_4$ [32], 2.575 Å in $Rb_2MnSe_2$ [33], and 2.571(7) Å in $Mn_8[BeSiO_4]_6Se_2$ [34].

It is useful to compare (Fig. 4) the $CeMn_{0.5}OSe$ structure with the intermetallic structure types CeFeSi [35] and $ThCr_2Si_2$ [36] (an ordered substitution variant of the $BaAl_4$ structure type). The main feature is the existence of a common block in these three layered structures. This block is defined by the Ce–Si–Fe–Si–Ce sequence in the CeFeSi structure, the Th–Si–Cr–Si–Th sequence in the $ThCr_2Si_2$ structure, and the Ce–Se–Mn–Se–Ce sequence in the $CeMn_{0.5}OSe$ structure, where Fe, Cr, and Mn are tetrahedrally coordinated to Si or Se atoms. This sequence has been denoted as a "$BaAl_4$" slab [37]. Therefore, the $ThCr_2Si_2$ structure is constituted from two juxtaposed $BaAl_4$ slabs along [001] whereas the CeFeSi structure is built from two $BaAl_4$ slabs with additional Ce–Ce interactions. In $CeMn_{0.5}OSe$ structure, the O layer is inserted between these two Ce layers 1.219 Å from each. Several other chalcogenide phases crystallize with the $ThCr_2Si_2$ structure type, namely $AM_2Q_2$ ($A$ = alkali or alkaline-earth metal; $M$ = 3$d$-transition metal; $Q$ = S, Se) [38,39], $ACuMnS_2$ ($A$ = K, Rb) [40], $CsCuFeS_2$ [41], and $KCuZnTe_2$ [42]. In an alternative description $CeMn_{0.5}OSe$ may be considered as an intergrowth structure consisting of two kinds of infinite slabs with square–mesh interfaces. The first slab with composition "$CeO_2$" is sliced from the binary oxide $CeO_2$ ($CaF_2$ structure type) The second slab with composition "$CeMn_{2-y}Se_2$" has an atomic arrangement that corresponds to the $ThCr_2Si_2$ structure. The only atoms positioned on the slab interfaces and shared between the intergrown slabs are the Ce atoms, an arrangement that has been catalogued [43].

### 3.3. Magnetism

Because of their interesting magnetic properties the Mn representatives of the CeFeSi and $ThCr_2Si_2$ structure types, namely $LnMnX$ and $LnMn_2X_2$ ($X$ = Si or Ge), have been extensively studied by macroscopic magnetic measurements, neutron diffraction, and Mössbauer spectroscopy. It has been found that magnetic ordering of the Mn sublattice appears to be correlated with the intra-layer Mn–Mn spacing [44–47]. In these compounds long Mn–Mn distances (> 2.86 Å) yield antiferromagnetic (001) Mn layers whereas shorter distances yield ferromagnetic Mn layers. The Mn sublattice in $CeMn_{0.5}OSe$ comprises (001) square planes,

with the Mn–Mn distance in this plane being 2.8465(5) Å. Disregarding the metallic nature of bonding in the CeFeSi and $ThCr_2Si_2$ structures and the partial occupancy of Mn in the present structure, the structural analogy among these phases is obvious. Unfortunately, the magnetic properties of $CeMn_{0.5}OSe$ remain unknown owing to our inability to prepare this material and other rare-earth representatives in sufficient amounts.

### 3.4. Band gap

The optical absorption spectrum and its second derivative vs. photon energy are displayed in Fig. 5 for light impinging on the (100) crystal face of a $CeMn_{0.5}OSe$ single crystal. Analysis leads to a band gap of 2.01 eV. The dark-orange color of $CeMn_{0.5}OSe$ is consistent with this band gap.

## Acknowledgments

This research was supported by the US National Science Foundation under Grant DMR00-96676 (J.A.I), a Ford Predoctoral Fellowship to K.M., and a Northwestern University Presidential Fellowship to C.L.H. Use was made of the MRL Central Facilities supported by the National Science Foundation at the Materials Research Center of Northwestern University under Grant No. DMR00-76097.

## References

[1] J.A. Cody, J.A. Ibers, J. Solid State Chem. 114 (1995) 406–412.
[2] C. Deudon, A. Meerschaut, L. Cario, J. Rouxel, J. Solid State Chem. 120 (1995) 164–169.
[3] J.A. Cody, C. Deudon, L. Cario, A. Meerschaut, Mater. Res. Bull. 32 (1997) 1181–1192.
[4] L.J. Tranchitella, J.C. Fettinger, B.W. Eichhorn, Chem. Mater. 8 (1996) 2265–2271.
[5] L. Cario, C. Deudon, A. Meerschaut, J. Rouxel, J. Solid State Chem. 136 (1998) 46–50.
[6] L.J. Tranchitella, J.C. Fettinger, S.F. Heller-Zeisler, B.W. Eichhorn, Chem. Mater. 10 (1998) 2078–2085.
[7] C. Boyer, C. Deudon, A. Meerschaut, C.R. Acad. Sci. Ser. IIc: Chim. 2 (1999) 93–99.
[8] M. Goga, R. Seshadri, V. Ksenofontov, P. Gütlich, W. Tremel, J. Chem. Soc. Chem. Commun. (1999) 979–980.
[9] O. Tougait, J.A. Ibers, Chem. Mater. 12 (2000) 2653–2658.
[10] V. Meignen, C. Deudon, A. Lafond, C. Boyer-Candalen, A. Meerschaut, Solid State Sci. 3 (2001) 189–194.
[11] O. Tougait, J.A. Ibers, J. Solid State Chem. 157 (2001) 289–295.
[12] J. Dugué, T. Vovan, P. Laruelle, Acta Crystallogr. Sect. C: Cryst. Struct. Commun. 41 (1985) 1146–1148.
[13] T. Vovan, J. Dugué, M. Guittard, C. R. Acad. Sci. Sér. 2 (292) (1981) 957–959.
[14] O. Tougait, J.A. Ibers, J. Solid State Chem. 154 (2000) 564–568.
[15] J. Dugué, T. Vovan, J. Villers, Acta Crystallogr. Sect. B: Struct. Crystallogr. Cryst. Chem. 36 (1980) 1291–1294.
[16] J. Dugué, T. Vovan, J. Villers, Acta Crystallogr. Sect. B: Struct. Crystallogr. Cryst. Chem. 36 (1980) 1294–1297.
[17] M. Wintenberger, T. Vovan, M. Guittard, Solid State Commun. 53 (1985) 227–230.
[18] T. Vovan, J. Dugué, M. Guittard, Mater. Res. Bull. 13 (1978) 1163–1166.
[19] M. Wintenberger, J. Dugué, M. Guittard, N.H. Dung, V.V. Tien, J. Solid State Chem. 70 (1987) 295–302.
[20] T.V. Van, D.N. Huy, C. R. Acad. Sci. Sér. 2 (293) (1981) 933–936.
[21] M. Palazzi, C. R. Acad. Sci. Sér. 2 (292) (1981) 789–791.
[22] W.J. Zhu, Y.Z. Huang, C. Dong, Z.X. Zhao, Mater. Res. Bull. 29 (1994) 143–147.
[23] A.M. Kusainova, P.S. Berdonosov, L.G. Akselrud, L.N. Kholodkovskaya, V.A. Dolgikh, B.A. Popovkin, J. Solid State Chem. 112 (1994) 189–191.
[24] P.S. Berdonosov, A.M. Kusainova, L.N. Kholodkovskaya, V.A. Dolgikh, L.G. Akselrud, B.A. Popovkin, J. Solid State Chem. 118 (1995) 74–77.
[25] F.Q. Huang, P. Brazis, C.R. Kannewurf, J.A. Ibers, J. Solid State Chem. 155 (2000) 366–371.
[26] Bruker, SMART Version 5.054 Data Collection and SAINT-Plus Version 6.22 Data Processing Software for the SMART System, Bruker Analytical X-ray Instruments, Inc., Madison, WI, USA, 2000.
[27] G.M. Sheldrick, SHELXTL DOS/Windows/NT Version 6.12, Bruker Analytical X-ray Instruments, Inc., Madison, WI, USA, 2000.
[28] L.M. Gelato, E. Parthé, J. Appl. Crystallogr. 20 (1987) 139–143.
[29] K. Mitchell, C.L. Haynes, A.D. McFarland, R.P. Van Duyne, J.A. Ibers, Inorg. Chem. 41 (2002) 1199–1204.
[30] M. Palazzi, S. Jaulmes, Acta Crystallogr. Sect. B: Struct. Crystallogr. Cryst. Chem. 37 (1981) 1337–1339.
[31] M. Grupe, W. Urland, Naturwissenschaften 76 (1989) 327–329.
[32] I.E. Grey, H. Steinfink, Inorg. Chem. 10 (1971) 691–696.
[33] W. Bronger, H. Balk-Hardtdegen, D. Schmitz, Z. Anorg. Allg. Chem. 574 (1989) 99–106.
[34] S.E. Dann, M.T. Weller, B.D. Rainford, D.T. Adroja, Inorg. Chem. 36 (1997) 5278–5283.
[35] O.I. Bodak, E.I. Gladyshevskii, P.I. Kripyakevich, Zh. Strukt. Khim. 11 (1970) 305–310.
[36] Z. Ban, M. Sikirica, Acta Crystallogr. 18 (1965) 594–599.
[37] E. Parthé, B. Chabot, Crystal structures and crystal chemistry of ternary rare earth-transition metal borides silicides and homologues, in: K.A. Gschneidner Jr., L. Eyring (Eds.), Handbook on the Physics and Chemistry of Rare Earths, Vol. 6, Elsevier Science Publishers B.V., New York, 1984, pp. 113–334.
[38] G. Huan, M. Greenblatt, M. Croft, Eur. J. Solid State Inorg. Chem. 26 (1989) 193.
[39] M. Saeki, M. Onoda, H. Nozaki, Mater. Res. Bull. 23 (1988) 603–608.
[40] M. Mouallem-Bahout, M. Potel, J.-F. Halet, J. Padiou, C. Carel, M. Retat-Savel'eva, Eur. J. Solid State Inorg. Chem. 33 (1996) 483–493.
[41] J. Llanos, P. Valenzuela, C. Mujica, A. Buljan, R. Ramírez, J. Solid State Chem. 122 (1996) 31–35.
[42] H.R. Heulings IV, J. Li, D.M. Proserpio, Main Group Met. Chem. 21 (1998) 225–229.
[43] E. Parthé, B.A. Chabot, K. Cenzual, Chimia 39 (1985) 164–174 (Fig. 8, Column 2).
[44] R. Welter, B. Malaman, G. Venturini, Solid State Commun. 108 (1998) 933–938.
[45] G. Venturini, B. Malaman, E. Ressouche, J. Alloys Compd. 240 (1996) 139–150.
[46] I. Ijjaali, R. Welter, G. Venturini, B. Malaman, E. Ressouche, J. Alloys Compd. 270 (1998) 63–72.
[47] I. Ijjaali, G. Venturini, B. Malaman, E. Ressouche, J. Alloys Compd. 266 (1998) 61–70.